

Ginzburg-Landau approach to inhomogeneous chiral phases of QCD

Hiroaki Abuki and Katsuhiko Suzuki

Department of Physics, Tokyo University of Science, Tokyo 162-8601, Japan

Abstract. We study the inhomogeneous chiral condensates in the proximity of the chiral tricritical point (TCP) of two-flavor QCD. Deriving the Ginzburg-Landau (GL) functional up to the eighth order in the order parameter and its spatial derivative, we explore off the TCP and find that critical curves are bent by non-linear effects. In the newly extend GL coupling space, we find the TCP being realized as a multicritical point where five independent critical lines meet up. We also present general analyses for the energies associated with several higher dimensional crystal structures.

Keywords: QCD, critical point, inhomogeneous phases, chiral symmetry

PACS: 12.38.Mh, 21.65.Qr, 25.75.Nq

Introduction. – Chiral condensates with possible crystal structures are of particular interest in the field of QCD under extreme conditions. Such a partial spatial breaking of quark-antiquark condensate may be driven by the quark chemical potential μ serving as an external field which favor to produce a net population excess of quarks over antiquarks. This was indeed proven to be true in the neighborhood of the chiral tricritical point (TCP) in Ref. [1] where the author took the advantage of the Ginzburg-Landau (GL) framework which is capable to make model independent predictions. TCP was found to be replaced by the Lifshitz point (LP) from which a solitonic chiral phase expands. Such phase structure is now known to survive after incorporating the effect of current quark mass [2] or Polyakov loop [3].

Most studies so far restrict the analyses to the one dimensional crystal structure mainly for technical reason, although such state is known to be fragile against thermal fluctuations [4]. Also moving off the TCP, we might expect other types of inhomogeneous states, including the chiral density wave [7], come into play and change the phase structure just as in the case of superconductivity under an external magnetic field [5].

In this article, we report the extended GL analyses for the chiral crystal phases near TCP in the chiral limit based on our recent paper [6]. We aim at the clarification of (1) how the inhomogeneous chiral condensate is deformed or taken over by other phases once departing from the TCP, (2) whether or not multidimensional crystal structures get favored over one-dimensional solitonic state, and finally (3) the structure of the TCP in a wider extended GL coupling space.

Extended Ginzburg-Landau approach. – In order to allow for a minimal description of the TCP and possible inhomogeneous states in its neighborhood, we need to expand the GL functional up to sixth order in the order parameter and its spatial derivative. The expression was found as [1]:

$$\omega = \frac{\alpha_2}{2} M(\mathbf{x})^2 + \frac{\alpha_4}{4} (M(\mathbf{x})^4 + (\nabla M)^2) + \frac{\alpha_6}{6} \left(M(\mathbf{x})^6 + 5M^2(\nabla M)^2 + \frac{1}{2}(\Delta M)^2 \right), \quad (1)$$

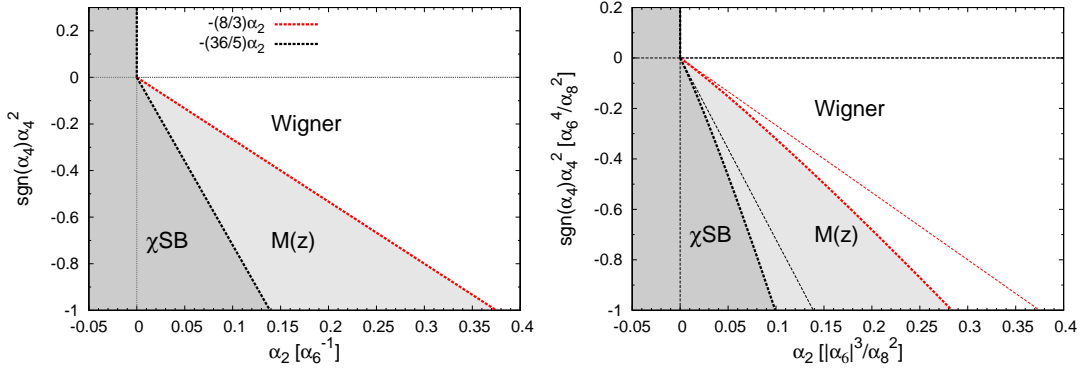


FIGURE 1. (Left panel): The GL phase diagram for Eq. (1), computed at the mean-field level with restricted to one-dimensional structures. (Right panel): The phase diagram after including the effect of eighth order terms, $\delta\omega$. For comparison, the critical lines enclosing the inhomogeneous phase in the absence of $\delta\omega$ (those in the left figure) are repeated by thin dashed lines.

where $M(\mathbf{x}) \sim \langle \bar{q}q(\mathbf{x}) \rangle$ is the chiral condensate, and α_2 , α_4 and α_6 are the relevant GL couplings. If $\alpha_6 > 0$, We can draw a phase diagram in the two dimensional GL parameter space (α_2, α_4) . It can be shown that the thermodynamics only depends on the sign of α_4 and dimensionless ratio $\alpha_4^2/(\alpha_2[\alpha_6^{-1}])$ where $\alpha_2[\alpha_6^{-1}]$ means $\alpha_2\alpha_6$, i.e., the value of α_2 measured in the unit of α_6^{-1} . Due to this scaling property, all the critical lines in the $(\alpha_2[\alpha_6^{-1}], \text{sgn}(\alpha_4)\alpha_4^2)$ -plane should be expressed as straight lines, and any two of them never intersect one another once departing from the origin. The phase diagram for this case is shown in the left panel of Figure 1. We find a Lifshitz TCP at the origin; the region labeled by $M(z)$ is the phase of inhomogeneous chiral condensate characterized by Jacobi's elliptic function $M(z) = \sqrt{k}v\text{sn}(kz, v)$ with v being the elliptic modulus.

Exploration off the TCP. – In order to explore a new phase structure which may show up away from the TCP within the GL framework, we need to go beyond the minimal GL described above. The term which should be added at eighth order is [6]

$$\delta\omega = \frac{\alpha_8}{8} (M^8 + 14M^4(\nabla M)^2 - \frac{1}{5}(\nabla M)^4 + \frac{18}{5}M\Delta M(\nabla M)^2 + \frac{14}{5}M^2(\Delta M)^2 + \frac{1}{5}(\nabla\Delta M)^2). \quad (2)$$

Coefficients appearing in front of each term are all proportional to α_8 , and can be extracted by evaluating the quark loop diagrams. α_8 should be positive for thermodynamic stability, while α_6 can be either positive or negative. We first focus on the case $\alpha_6 > 0$ which has close connection to the analysis at the sixth order, and later come back to the case $\alpha_6 < 0$. With inclusion of this $\delta\omega$, we can see that the thermodynamics now is a function of two independent parameters, α_2 and α_4 . In the right panel of Figure 1, the phase diagram is depicted in the $(\alpha_2, \text{sgn}(\alpha_4)\alpha_4^2)$ -plane. In this case two critical lines surrounding the phase are bent by the nonlinear effect from the eight order terms. In fact it is possible to derive the following expansions for the formation of single soliton (the dashed curve on the left side) and for the melting of condensate (the one on the right

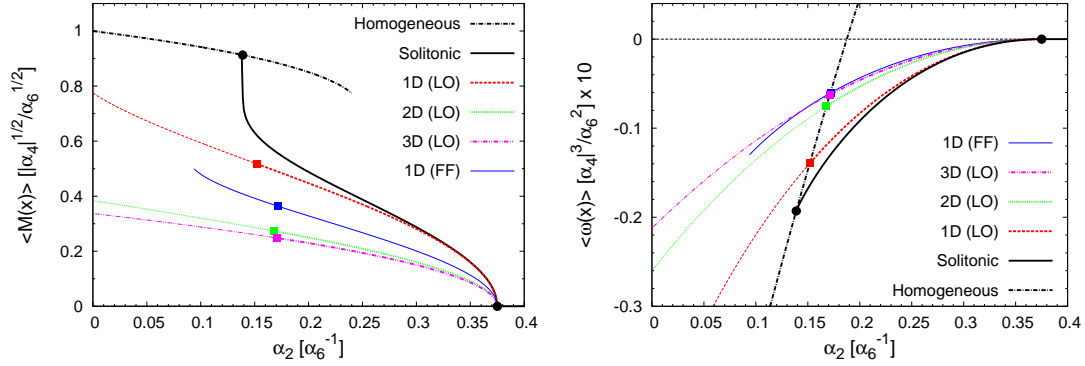


FIGURE 2. The comparison of spatial average of order parameter (Left) and that of functional potential density (Right) for several states along the section $\alpha_4 = -1$ in the left figure of Figure 1.

side, red online):

$$\begin{aligned} \alpha_2 &= \frac{5}{36} \alpha_4^2 \left(1 + \frac{25}{42} \alpha_8 \alpha_4 + \frac{625}{784} (\alpha_8 \alpha_4)^2 + \mathcal{O}((\alpha_8 \alpha_4)^3) \right), \\ \alpha_2 &= \frac{3}{8} \alpha_4^2 \left(1 + \frac{9}{20} \alpha_8 \alpha_4 + \frac{729}{1600} (\alpha_8 \alpha_4)^2 + \mathcal{O}((\alpha_8 \alpha_4)^3) \right). \end{aligned} \quad (3)$$

Here α_2 and α_8 in the above formulas mean $\alpha_2[\alpha_6^{-1}]$ and $\alpha_8[\alpha_6^2]$ respectively. However, apart from these nonlinear bending of critical lines, no new phase structure appears.

Multidimensional crystal structures? – We have limited the above analyses to the condensate having its spatial modulation only in one direction, i.e., one-dimensional modulation. With this restriction, it is possible to solve the Euler-Lagrange equation analytically leading to results demonstrated in Figure 1. Here we lift the limit, and explore the possibility of multidimensional crystal structures using a variational method. The states we consider are the extensions of one-dimensional Larkin Ovchinnikov (LO)-type condensate ($M_{1D-LO}(\mathbf{x}) = \sqrt{2}M_0 \sin(kz)$) to higher dimensions,

$$\begin{aligned} M_{2D-LO}(\mathbf{x}) &= M_0(\sin(kx) + \sin(ky)), \\ M_{3D-LO}(\mathbf{x}) &= \sqrt{\frac{2}{3}}M_0(\sin(kx) + \sin(ky) + \sin(kz)), \end{aligned} \quad (4)$$

where k and M_0 are to be optimized for each state. Figure 2 shows the comparison of the spatial average of order parameter $\langle M(\mathbf{x}) \rangle$ (Left panel) and the averaged potential $\langle \omega(\mathbf{x}) \rangle$ (Right panel) for the several states along the section $\alpha_4 = -1$ in the left panel of Figure 1. “FF” refers to the Fulde-Ferrell (FF)-like state characterized by $M_{1D-FF}(\mathbf{x}) = M_0 e^{ikz}$ in which the time-reversal symmetry as well as rotational symmetry is broken. We see that the magnitude of condensate is decreasing function of dimensionality and the energy density is accordingly in the opposite tendency. Similar results for two dimensional condensates at $T = 0$ were recently obtained in the NJL model [8, 9]. The inclusion of eighth order terms in $\delta\omega$ does not change this situation so that one-dimensional solitonic state is most favorable for all values of $\alpha_8\alpha_4$.

We can derive the analytic formulas for the dependence of free energy on the number of spatial directions in which the condensate varies by expanding the GL functional in

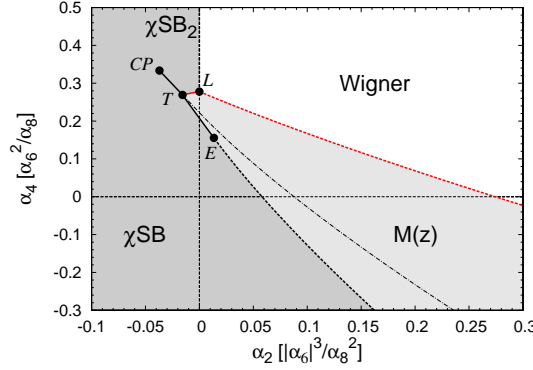


FIGURE 3. The GL phase diagram for $\alpha_6 < 0$ computed from Eq. (1). Dashed lines express the second order phase boundaries, while full lines do the first order ones. Dot-dashed line in the inhomogeneous phase represents the first order phase transition which would have been realized if the inhomogeneous phase was not taken into consideration.

the vicinity of condensate-melting line. We first set the higher (d-)dimensional analog of the LO and FF states as

$$M_{\text{dD-FF}}(\mathbf{x}) = \frac{1}{\sqrt{d}} M_0 (e^{ikx_1} + e^{ikx_2} + \dots + e^{ikx_d}),$$

$$M_{\text{dD-LO}}(\mathbf{x}) = \sqrt{\frac{2}{d}} M_0 (\sin(kx_1) + \sin(kx_2) + \dots + \sin(kx_d)).$$
(5)

Then at the proximity of the line of vanishing condensate, we arrive at the following analytic formulas for $\langle \omega(\mathbf{x}) \rangle$ via expanding in M_0 after optimizing the wavevector k over M_0 :

$$\langle \omega_{\text{dD-LO}}(\mathbf{x}) \rangle = \left(\frac{\alpha_2}{2} - \frac{3}{16} \alpha_4^2 \right) M_0^2 + \frac{2d-1}{4d} M_0^4 + \mathcal{O}(M_0^6),$$

$$\langle \omega_{\text{dD-FF}}(\mathbf{x}) \rangle = \left(\frac{\alpha_2}{2} - \frac{3}{16} \alpha_4^2 \right) M_0^2 + \frac{1}{2} M_0^4 - \frac{4d^2+10d-7}{12d^2} M_0^6 + \mathcal{O}(M_0^8).$$
(6)

From these we see that, in the case of LO-type condensates the energy density is in the order of dimensionality of spatial modulation. In the FF case, the difference becomes visible only at sextic order, and the dependence on dimensionality is not monotonic; the 2D structure is most favorable within this class of condensates. From these analyses we find that increasing the directions of spatial modulation is accompanied by a large kinematical energy cost, leading to the conclusion that multidimensional crystals are unlikely to be realized in the neighborhood of the TCP.

The structure of TCP. – We now explore a new regime $\alpha_6 < 0$. The corresponding phase diagram is depicted in Figure 3. We see that the Lifshitz tricritical point for $\alpha_6 > 0$ splits into four multicritical points; the critical point (CP), the Triple point (T), the Lifshitz bicritical point (L), and the critical endpoint (E). Their (α_2, α_4) -coordinates are listed in TABLE 1. All these points scale as $(\#|\alpha_6|^3/\alpha_8^2, \#\alpha_6^2/\alpha_8)$ so that they are all going to degenerate into the origin as $\alpha_6 \rightarrow 0^-$, smoothly continuing to the Lifshitz TCP in the positive α_6 side. Among these critical points the most intriguing is T where three first order phase transitions meet. At this point, three different forms of broken-symmetry

TABLE 1. The coordinates of locations of the multicritical points.

Label	Type	Coordinate (α_4 [α_6^3/α_8^2], α_2 [α_6^2/α_8])	
CP	Critical point	($-1/27, 1/3$)	(analytical)
T	Triple point	($-0.016, 0.27$)	(numerical)
L	Lifshitz bicritical point	($0, 5/18$)	(analytical)
E	Critical endpoint	($0.014, 0.16$)	(numerical)

phase compete and coexist. These are; the state with homogeneous chiral condensate, the state with smaller chiral condensate denoted by “ χSB_2 ”, and the inhomogeneous chiral condensate labeled by $M(z)$. It is possible to extract numerically the dimensionless ratios of physical quantities that are to be realized when the point **T** is approached:

$$\lim_{(\alpha_2, \alpha_4) \rightarrow T} \left\{ \frac{M(\chi\text{SB}_2)}{M(\chi\text{SB})}, \frac{\sqrt{\langle M(z)^2 \rangle}}{M(\chi\text{SB})}, \frac{2\pi/\ell_P}{\sqrt{\langle M(z)^2 \rangle}} \right\} = \{0.369, 0.308, 5.001\}, \quad (7)$$

where ℓ_P is the modulation period. These ratios characterize the triple point (**T**) and they are universal and model-independent in the sense that they do not depend on any of GL parameters including the magnitude of $|\alpha_6|$, and α_8 .

Summary. – In conclusion, we explored off the TCP based on the GL functional expanded up to eighth order in chiral order parameter and its spatial derivative. As a consequence, we found that the critical lines surrounding the inhomogeneous phase are bent because of the nonlinear effect coming from eight order terms although the qualitative phase structure remains unaffected. We also examined the possibility of higher dimensional crystal phase, but it turned out that the kinematical cost to make the condensate modulated in several directions is so high that it is unlikely to have multidimensional chiral crystals near the TCP. Finally we extended our analyses to a new regime $\alpha_6 < 0$. We found that the TCP splits into four multicritical points. It would be interesting to search for a thermodynamic physical quantity in QCD to which α_6 is sensitive. The isospin chemical potential or the chiral chemical potential might serve as one of such sources. The investigations in these directions deserve further efforts in future [10].

Acknowledgments. – H. A. thanks the organizers of QCD@Work2012 for giving him an opportunity to give a talk. The authors thank D. Ishibashi for the fruitful collaboration.

REFERENCES

1. D. Nickel, Phys. Rev. Lett. **103**, 072301 (2009) [arXiv:0902.1778 [hep-ph]].
2. D. Nickel, Phys. Rev. D **80**, 074025 (2009) [arXiv:0906.5295 [hep-ph]].
3. S. Carignano, D. Nickel and M. Buballa, Phys. Rev. D **82**, 054009 (2010) [arXiv:1007.1397 [hep-ph]].
4. G. Baym, B. L. Friman and G. Grinstein, Nucl. Phys. B **210**, 193 (1982).
5. S. Matsuo, S. Higashitani, Y. Nagato, and K. Nagai, J. Phys. Soc. Jpn. **67**, 280 (1998).
6. H. Abuki, D. Ishibashi and K. Suzuki, Phys. Rev. D **85**, 074002 (2012) [arXiv:1109.1615 [hep-ph]].
7. E. Nakano and T. Tatsumi, Phys. Rev. D **71**, 114006 (2005) [hep-ph/0411350].
8. S. Carignano and M. Buballa, arXiv:1111.4400 [hep-ph].
9. S. Carignano and M. Buballa, arXiv:1203.5343 [hep-ph].
10. Y. Iwata, H. Abuki and K. Suzuki, arXiv:1206.2870 [hep-ph].